

Study on Corrosion Behavior of HDR Duplex Stainless Steel Welded Joints

Xin Liu^{1,a}, Chaojun Yang^{2,b} and Nian Liu^{3,*}

¹Naval University of Engineering, Wuhan 430033, China;

²Wuhan University of Science and Technology, Wuhan 430081, China;

³Navy 91844 troops, Guangzhou 510000, China.

^aliuxin2008dragon@126.com, ^by1123001016@163.com,

*Corresponding author email: 18162626365@163.com

Abstract. Aiming at the actual corrosion problem of HDR duplex stainless steel used in marine seawater system, this paper studies the corrosion behavior of welded joints. The corrosion behavior of welded joints was studied by means of microstructure analysis, potentiodynamic polarization experiment and double-ring potentiodynamic reactivation experiment, and the influence of welding process parameters on the corrosion resistance of HDR duplex stainless steel welded joints was investigated. The results show that: (1) The backing welding current has obvious influence on the microstructure of weld metal of HDR steel. The grains in the lower part of the weld are smaller, the quantity is high. (2) The backing welding current has obvious influence on the microstructure of the heat affected zone of HDR steel welded joint, and heat treatment promotes the transformation from ferrite to austenite in the heat affected zone. (3) The ratio of two phases is closer to 1, and the weld metal has better intergranular corrosion resistance in DL-EPR experiment; When the chromium content is low, the intergranular corrosion resistance of weld metal is poor; With the increase of welding gap, the Ra value of weld metal increases gradually, and the intergranular corrosion sensitivity increases gradually.

Keywords: Welding parameter; HDR Duplex Stainless Steel; Structure; Corrosion Behavior.

1. Introduction

Water cooling system is an indispensable and important part of the production process in many industrial fields, such as shipbuilding, electric power, oil refining, chemical industry and so on. At present, the commonly used material of marine seawater system is copper alloy. Due to the lack of corrosion performance of copper alloy in flowing seawater, marine seawater system often corrodes, and duplex stainless steel has good performance in flowing seawater, which has also been applied in the marine field. The corrosion resistance of duplex stainless steel is closely related to the microstructure [1-3]. In practical use, improper processing, welding and other treatments will cause problems such as phase imbalance and harmful secondary phase precipitation, which will reduce the corrosion resistance and cause corrosion problems [4-6].

Aiming at the actual corrosion problem of HDR duplex stainless steel used in marine seawater system, this paper studies the corrosion behavior of welded joints. The corrosion behavior of welded joints was studied by analyzing the composition and microstructure of welded joints and related corrosion experiments, and the influence of welding process parameters on the corrosion resistance of HDR duplex stainless steel welded joints was investigated.

2. Materials And Experimental Methods

2.1 Material

The material used in this experiment is HDR duplex stainless steel pipe produced by Shanghai Shisheng Technology Development Co., Ltd., and the welding wire is HDR. The chemical composition of special welding wire, welding wire and stainless steel tube is shown in Table 1.

Table 1 Chemical compositions of materials (mass fraction) (wt%)

Element	Cr	Ni	C	Mo	Si	P	S	N	Mn
HDR	24.54	5.82	0.026	2.15	0.42	0.021	0.001	0.168	1.26
solder wire	24.73	6.83	0.03	2.09	0.31	0.018	0.005	0.2	1.13

2.2 Welding Experiment

According to the thickness of base metal and the diameter of welding wire, backing weld used $\Phi 1.5$ mm welding wire to weld three groups of samples. The specific welding process parameters and sample numbers are shown in Table 2.

Table 2 Welding parameter

Sample No.	welding current/A	interpass temperature/ $^{\circ}$ C	Welding gap/mm
1#	65	130-150	2.0
2#	70	130-150	2.0
3#	75	130-150	2.0

2.3 Microstructure Analysis of Welded Joint

AURIGA scanning electron microscope (SEM) was used to observe and analyze the microstructure of the samples, and IPP software was used to calculate the austenite content in different samples and different regions of the same sample. Energy dispersive spectrometer (EDS) was used to analyze the components of ferrite, austenite and precipitated phase in the samples.

2.4 Test of Potentiodynamic Polarization Curve

Welding a copper wire on the opposite side of the test surface, encapsulating the sample with epoxy resin, smoothing the test surface with 180#, 400#, 800#, 1000#, 1200#, 1500# and 2000# water sandpaper in turn, polishing it with diamond grinding paste, cleaning it with deionized water, acetone and anhydrous ethanol, drying it and placing it in a drying dish for later use.

According to GB/T 17899-1999 Method for Measuring Pitting Corrosion Potential of Stainless Steel, the polarization curves of dynamic potential of HDR duplex stainless steel welded joints were measured, and the pitting corrosion resistance of welded joints was compared and analyzed.

2.5 Test of Bicyclic Potentiodynamic Potential

In order to analyze the intergranular corrosion resistance of welded joints of HDR steel, the base metal, weld metal and heat affected zone were tested by double-ring potentiodynamic reactivation method. The experimental instrument is CS310H electrochemical workstation, and the experimental temperature is 30 $^{\circ}$ C. The maximum currents I_a and I_r of the anodized ring and the reactivation ring of the sample were measured, and R_a was used as a measure to evaluate the intergranular corrosion resistance of the sample. The greater R_a , the worse the intergranular corrosion resistance of the sample.

3. Result Analysis

3.1 Microstructure

The etching methods of HDR steel were compared and studied. The microstructure of welded joint samples prepared under different welding current conditions was analyzed by scanning electron microscope, and the influence of backing welding current on the microstructure of welded joint samples was analyzed and studied. The backing welding currents of the three samples are 65A, 70A and 75A, respectively, and the cover welding current is 100A. 1#, 2#, 3# weld metal samples of SEM morphology and energy spectrum analysis diagram as shown in Fig.1.

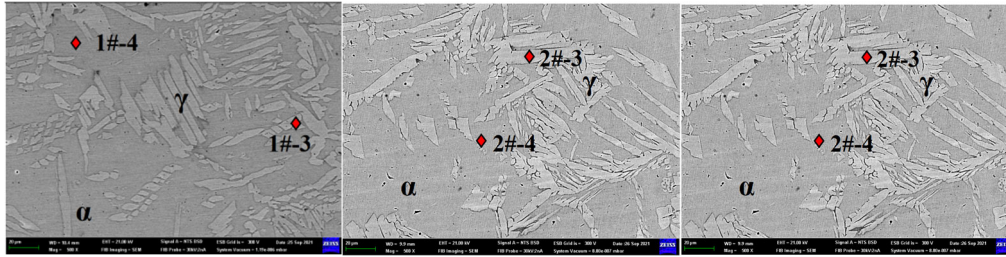


Fig. 1 Sem morphology of samples 1 #, 2 #, and 3 #

The two-phase ratio and composition analysis of weld metal and base metal under different backing welding currents are summarized in Table 3.

Table 3 Contents of main alloying elements of HDR steel welds under different base welding currents

Sample No.	phase structure	volume(%)	Cr(wt.%)	Mo(wt.%)	Ni(wt.%)
1#-WM-X	austenite	44.94	24.87	1.93	7.72
	ferrite	55.06	25.76	2.43	6.79
2#-WM-X	austenite	49.74	25.21	1.99	7.46
	ferrite	50.26	25.67	2.44	6.87
3#-WM-X	austenite	53.46	24.97	1.81	7.47
	ferrite	46.54	25.65	2.27	6.68

In duplex stainless steel, the distribution of alloying elements such as Cr, Mo and Ni will be gradually homogenized with the increase of temperature. With the decrease of temperature, ferrite stabilizing elements such as Cr and Mo tend to segregate into ferrite, while Ni tends to segregate into austenite, which eventually leads to the difference in the distribution of alloying elements in the two phases. Generally speaking, the higher the welding heat input, the lower the cooling rate of weld, Cr, the segregation phenomenon of alloying elements such as Mo and Ni is more obvious. In addition, due to the heat treatment effect of the second welding on the first welding, Cr, Mo and other elements at the lower part of the welding seam are further concentrated in ferrite, while Ni is further concentrated in austenite.

3.2 Analysis of Potentiodynamic Polarization Curve

The anodic polarization curve of the sample was measured by potentiodynamic scanning, and the scanning was stopped when the current density reached $1\text{mA}/\text{cm}^2$. The polarization curves of weld metal and parent metal samples of HDR steel are shown in Fig.4. Take the potential corresponding to the current density of $100\mu\text{A}/\text{cm}^2$ as the pitting potential E_b of the sample, and the E_b measured from the polarization curve is shown in Table 4.

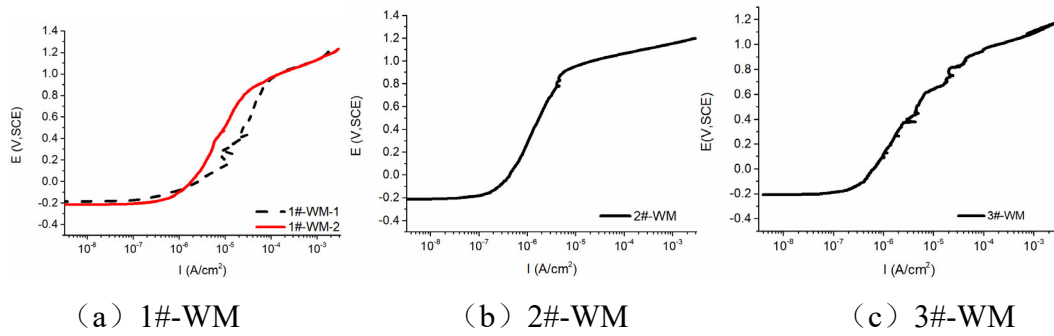


Fig. 2 Polarization curves of weld and base metal

Table 4 Main characteristic values of polarization curves of base metal and weld

Sample No.	BM-1	BM-2	1#-WM-1	1#-WM-2	2#-WM-1	3#-WM-1
E _b (V)	1.051	1.042	0.955	0.965	1.027	0.960

As can be seen from Table 4, the pitting corrosion potential of weld metal samples 1#, 2# and 3# is lower than that of the base metal, and the current in the passivation zone is obviously higher than that of the base metal, indicating that the passivation film performance and pitting corrosion resistance of these three weld metal samples are lower than that of the base metal. The pitting corrosion potentials of sample 1# and sample 3# are similar, and they are obviously lower than those of sample 2#, which shows that the pitting corrosion resistance of sample 2# is better than that of sample 1# and sample 3#. From the perspective of microstructure, the ratio of two phases in sample 2# is closer to 1, and the difference of alloy element content between the two phases is also small.

3.3 Results of Reactivation of Double-ring Potentiodynamic Potential

DL-EPR was used. First, it was polarized at a constant potential of 0.9V below the open circuit potential for 5 minutes to remove the passive film on the surface of the sample. After the potential stabilized, it was scanned forward from the open circuit potential to 0.7V(vs.OCP) at a speed of 1.5mV/s, and then swept back to the open circuit potential at the same rate. The experimental curve is shown in Fig.3.

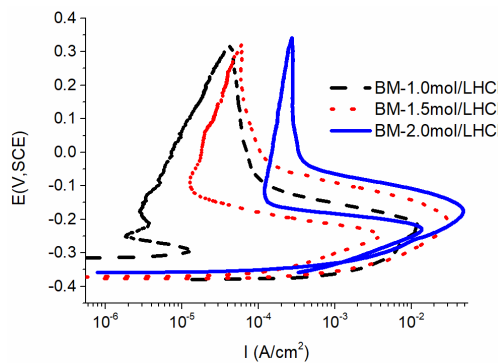


Fig. 3 Influence of hydrochloric acid concentration on dlepr test

As can be seen from Figure 4, the concentration of hydrochloric acid has a significant influence on the reactivation peak current I_r of samples. When the concentration is 1.0mol/L, the depolarization effect of hydrochloric acid is too weak, the reactivation peak current I_r is very small, the R_a is very small, and the difference of R_a values of different samples is small, so it is not easy to compare their intergranular corrosion resistance. When the concentration of hydrochloric acid is 2.0 mol/L, the depolarization effect of HCl is too strong, the peak reactivation current I_r is large, and the R_a values of the samples are all large. It is also difficult to compare the intergranular corrosion resistance of different samples. When the concentration of hydrochloric acid is 1.5 mol/L, the R_a values of different samples are obviously different, which is convenient to compare the intergranular corrosion sensitivity of weld metal with base metal and different welding parameters. Therefore, the DL-EPR

experiment in this study adopts 2.0mol/L H₂SO₄ and 1.5mol/L HCl system for subsequent experiments.

The DL-EPR experimental curve of weld metal and base metal samples with 2.0mol/L H₂SO₄ and 1.5mol/L HCl system is shown in Fig.4, and R_a values of the base metal and weld in TABLE 5.

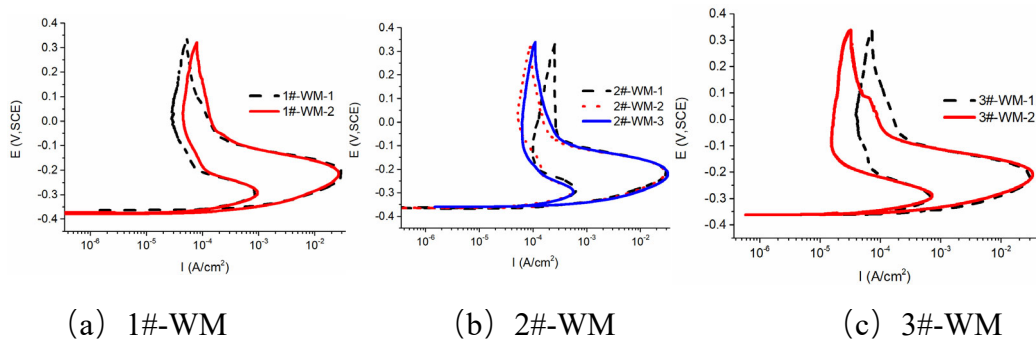


Fig. 4 DL-EPR curves of base metal and weld

Table 4 R_a values of the base metal and weld

Sample No.	BM	1#	2#	3#
R _a	12.39%	2.52%	1.92%	2.21%

As can be seen from Table 5, the R_a values of base metal and weld are both greater than 1%, which indicates that the sensitivity of base metal and weld to intergranular corrosion is greater in the acidic system used in the experiment. Compared with the weld, the R_a value of the base metal is the largest, which shows that the intergranular corrosion resistance of the base metal is lower than that of the weld in the system of 2.0mol/L H₂SO₄ and 1.5mol/L HCl.

4. Summarize

In this chapter, the self-corrosion potential, potentiodynamic polarization curve and double-ring potentiodynamic reactivation experiments were carried out on weld metal samples of HDR steel with different welding currents in 3.5%NaCl solution. The results are as follows:

- (1)The backing welding current has obvious influence on the microstructure of weld metal of HDR steel, the lower weld has smaller grains and higher austenite content.
- (2)Heat treatment can promote the transformation from ferrite to austenite in the heat affected zone and increase the backing welding current, which can improve the austenite content in the heat affected zone.
- (3)The microstructure of weld metal has obvious influence on pitting corrosion resistance. Two-phase ratio of sample 2# is closer to 1, and its pitting corrosion resistance is better.
- (4)With the increase of welding gap, the R_a value of weld metal increases gradually, and the intergranular corrosion sensitivity increases gradually.

Acknowledgments

Supporting projects: Naval Engineering University's Independent Research and Development Program, Research on Corrosion Behavior of HDR Dual Phase Stainless Steel Seawater Pipeline(Fund number:425317T005).

References

- [1] SILVA D D S, SIMÕES T A, MACEDO D A, et al. Microstructural influence of sigma phase on pitting corrosion behavior of duplex stainless steel/NaCl electrolyte couple[J]. Materials Chemistry & Physics, 2021, 259: 124056.

- [2] HA H-Y, LEE T-H, LEE C-G, et al. Understanding the relation between pitting corrosion resistance and phase fraction of S32101 duplex stainless steel[J]. Corrosion Science, 2019, 149: 226-235.
- [3] HA H-Y, JANG M-H, LEE T-H, et al. Interpretation of the relation between ferrite fraction and pitting corrosion resistance of commercial 2205 duplex stainless steel[J]. Corrosion Science, 2014, 89: 154-162.
- [4] XIAO Q, JANG C, KIM C, et al. Corrosion behavior of stainless steels in simulated PWR primary water: The effect of composition and matrix phases[J]. Corrosion Science, 2020, 177: 108991.
- [5] MURKUTE P, PASEBANI S, ISGOR B O. Effects of heat treatment and applied stresses on the corrosion performance of additively manufactured super duplex stainless steel clads[J]. Materialia, 2020, 14: 100878.
- [6] YANG Y, ZENG H T, XIN S S, et al. Electrochemical corrosion behavior of 2205 duplex stainless steel in hot concentrated seawater under vacuum conditions[J]. Corrosion Science, 2020, 165: 108383.